

Cytotoxicity of Polypropylenimine Dendrimer Conjugates on Cultured Endothelial Cells

Nathan A. Stasko,[†] C. Bryce Johnson,[‡] Mark H. Schoenfisch,[†] Timothy A. Johnson,[§] and Ekhsun L. Holmuamedov^{*,‡}

Department of Chemistry and Department of Cell and Developmental Biology, University of North Carolina at Chapel Hill, Chapel Hill, North Carolina 27599, and Department of Internal Medicine, East Carolina University, Greenville, North Carolina 27834

Received July 25, 2007; Revised Manuscript Received September 6, 2007

The cytotoxicity and time-dependent membrane disruption by polypropylenimine dendrimer conjugates on cultured human umbilical vein endothelial cells (HUVEC) is reported. Fluorescently labeled derivatives of generation 5 polypropylenimine dendrimers were prepared via conversion of amines to acetamides or through the covalent attachment of high molecular weight poly(ethylene glycol) (PEG) chains. Direct interactions between the fluorescent dendrimer conjugates and HUVEC were monitored using confocal fluorescence microscopy to track dendrimer movement across the plasma membrane and the fluorescent staining of cell nuclei. Propidium iodide and lactate dehydrogenase cytotoxicity assays confirmed that chemical modification of the surface amines of the parental dendrimer to neutral acetamide or PEG functionalities eliminated their acute cytotoxicity. Cationic primary-amine-containing dendrimers demonstrated drastic time-dependent changes in the plasma membrane permeability and prominent cytotoxicity. However, complete removal of the primary amines or masking of the cationic surface via PEGylation decreased dendrimer cytotoxicity. Thus, preventing electrostatic interactions of dendrimers with cellular membranes apparently is a necessary step toward minimizing the toxicity of delivery vehicles to the endothelium.

Introduction

Dendrimers are a new class of polymeric drug delivery vehicles that possess a well-defined, three-dimensional structure and a multivalent exterior which can be modified to contain a multitude of unique surface groups.^{1,2} These hyperbranched molecules are synthesized either by a divergent method whereby repeat monomers are branched outward from a central core or by a convergent method from which the synthesis begins at the periphery and is grown inward.³ The dendritic architecture offers a solution to traditional drug delivery problems by allowing for the tailored solubility and tissue-specific targeting of drugs through ligand or antibody immobilization to the multivalent surface.^{4,5} Recently, dendrimers have been employed as a substrate for delivering a wide range of therapeutic agents including water-insoluble drugs,^{6,7} anticancer chemotherapeutics,^{8–10} and oligonucleotides for enhanced gene transfection.¹¹

Some of the most promising nonviral gene delivery systems are dendritic structures with cationic amine exteriors, namely, the polyamidoamine (PAMAM) and polypropylenimine (PPI) dendrimers.¹² These synthetic vector systems form nucleic acid/dendrimer complexes through the interaction of cationic dendrimer exteriors with the negatively charged phosphates on the DNA backbone. Since Haensler et al. first reported the use of PAMAM dendrimers to mediate efficient gene transfection in vitro,¹³ numerous reports have explored the use of dendrimers as gene delivery vehicles, carefully detailing transfection efficiency as a function of carrier size, surface charge,

and exterior functionality.^{11,14–17} Although cationic amine-terminated dendrimers are suitable carriers to enhance gene transfection, the toxicity of these novel delivery vehicles and their unfavorable interactions with cellular membranes have slowed their widespread clinical application.¹¹ Indeed, Duncan et al. recently reviewed the toxicity of amine-containing dendrimers and concluded that amine-terminated dendrimers (e.g., PPI, PAM-AM) exhibited size-dependent cytotoxic effects based on the number of free amines at the surface.¹⁸ To further elucidate the mechanism of primary amine dendrimer toxicity, Hong et al. demonstrated that positively charged amine-terminated dendrimers induced the formation of nanoscale holes upon interaction with artificial lipid bilayers.¹⁹ Possible mechanisms of hole formation include dendrimer-mediated removal of lipids from the membrane²⁰ or direct insertion of the amine-terminated dendrimers into the membrane.²¹ Several other studies have been conducted illustrating that both negatively charged and neutral dendrimers were nontoxic, clearly demonstrating the structure/toxicity relationship that is governed primarily by the functional groups on the dendrimer surface.^{18,22–26}

In this report, we aimed to evaluate the cytotoxic effects of model dendritic systems against human umbilical vein endothelial cells (HUVEC) and provide further mechanistic insight into the structure/toxicity relationship of multifunctional polypropylenimine dendrimers. Time-dependent changes in the plasma membrane permeability of HUVEC toward propidium iodide (PI) and the concomitant release of cytosolic LDH were used to quantify cytotoxicity. Laser scanning confocal microscopy was employed to monitor both the interaction of fluorescently labeled dendrimers with the plasma membrane of HUVEC and the effect of dendrimer adhesion on the membrane potential of intracellular mitochondria. Chemical modification of the surface amines on the parent dendrimer and conversion to neutral

* Corresponding author: e-mail, ekhsun@med.unc.edu; tel, 919-966-5507; fax, 919-966-7197.

[†] Department of Chemistry, University of North Carolina at Chapel Hill.

[‡] Department of Cell and Developmental Biology, University of North Carolina at Chapel Hill.

[§] Department of Internal Medicine, East Carolina University.

acetamide or poly(ethylene glycol) functionalities reduced both the visible adhesion of dendrimers to the plasma membrane of cultured HUVEC and their cytotoxicity, illustrating that removal of the cationic charges from the dendrimer's surface is a necessary step in the synthesis of fully biocompatible drug-delivery vehicles.

Experimental Section

General Information. Tetramethylrhodamine methyl ester (TMRM) was purchased from Molecular Probes (Eugene, OR). Polypropyleneimine dendrimer (DAB-Am-64) starting material, propidium iodide (PI), poly(ethylene glycol) monomethyl ether (M-PEG₂₀₀₀), Kaiser test kit, and all other reagents were purchased from the Aldrich Chemical Co. (Milwaukee, WI). Methanol was distilled over magnesium prior to use. Water was purified with a Millipore Milli-Q gradient A-10 purification system (Bedford, MA). Spectra/Por Float-A-Lyzers were purchased from Spectrum Laboratories, Inc. (Rancho Dominguez, CA). Nuclear magnetic resonance (NMR) spectra were collected in deuterated water (D₂O) using a 400 MHz Bruker nuclear magnetic resonance spectrometer (Bruker, Germany). Mass spectra were acquired using a Micromass Quattro II triple quadrupole mass spectrometer equipped with a nanoelectrospray ionization source in positive-ion mode. Absorption spectra were recorded on a Perkin-Elmer Lambda 40 UV-vis spectrophotometer (Norwalk, CT). Fluorescence measurements were performed using a FluoStar Galaxy plate reader (BMG Lab Technologies, Inc., Durham, NC). Confocal fluorescence microscopy experiments were performed using an LSM 510 laser scanning confocal microscope (Carl Zeiss, Thornwood, NY).

Synthesis and Characterization of Dendrimer Conjugates.
DAB-Ac₄₀-FITC₂ (1). DAB-Am-64 (300 mg, 0.042 mmol) was dissolved in 30 mL of anhydrous methanol under an inert argon atmosphere, and to the stirring solution was added acetic anhydride (126 μ L, 1.34 mmol) and pyridine (119 μ L, 1.47 mmol) to stoichiometrically convert half of the primary amines on the dendrimer to acetamide functionalities. The solution was stirred for 24 h, and then 10 mL of anhydrous methanol containing fluorescein isothiocyanate (FITC) (49 mg, 0.126 mmol) was added to stoichiometrically attach three fluorescent residues per dendrimer. The solution was stirred for an additional 24 h in the dark and then separated into several aliquots for purification or further functionalization. Five milliliters of the product solution was concentrated under reduced pressure, dissolved in water, and added to a Spectra/Por Float-A-Lyzer (5 mL, 1000 MWCO) for dialysis in 2 L of 0.5 M NaCl for 24 h, followed by dialysis in ultrapure Milli-Q water for 3 days (3 \times 2 L). The aqueous sample was frozen and lyophilized to yield 21 mg of an orange solid: ¹H NMR (D₂O, δ): 1.2–1.70 (m, NCH₂CH₂CH₂N, NCH₂CH₂CH₂CH₂N), 1.80 (s, COCH₃), 1.86 (s, COCH₃), 2.07–2.54 (m, NCH₂CH₂CH₂N, NCH₂CH₂CH₂NH), 2.72 (m, NCH₂CH₂CH₂NH₂), 2.91 (m, NCH₂CH₂CH₂NHCOCH₃), 3.04 (m, NCH₂CH₂CH₂NHCOCH₃). ESI-MS calculated MW 9121.4 g/mol, experimental MW_{av} 9624.9 g/mol [1190.9 (M + 8H)⁸⁺, 1386.1 (M + 7H)⁷⁺, 1615.4 (M + 6H)⁶⁺]. UV/vis (MeOH): λ_{mac} = 504 nm.

DAB-Ac₅₉-FITC₂ (2). Acetic anhydride (32 μ L, 0.34 mmol) and pyridine (27 μ L, 0.34 mmol) were added to 5 mL of product solution containing dendrimer **1** to fully acetylate the remaining primary amines on the fluorescently labeled dendrimer. The solution was stirred for 24 h in the dark, concentrated under reduced pressure, resuspended in water, and dialyzed against 2 L of 0.5 M NaCl for 24 h, followed by dialysis in ultrapure Milli-Q water for 3 days (3 \times 2 L). The aqueous sample was frozen and lyophilized to yield 26 mg of an orange solid: ¹H NMR (D₂O, δ): 1.4–1.70 (m, NCH₂CH₂CH₂N, NCH₂CH₂CH₂CH₂N), 1.84 (s, COCH₃), 2.2–2.62 (m, NCH₂CH₂CH₂N, NCH₂CH₂CH₂NH), 3.03 (m, NCH₂CH₂CH₂NHCOCH₃). ESI-MS calculated MW 10425 g/mol, experimental MW_{av} 10,206 g/mol [1702.0 (M + 6H)⁶⁺, 2041.9 (M + 5H)⁵⁺, 2552.7 (M + 4H)⁴⁺]. UV/vis (MeOH) λ_{mac} = 504 nm.

4-Nitro-phenyl-MPEG. (Adapted from Kojima et al.²⁷). Poly(ethylene glycol) monomethyl ether (MPEG₂₀₀₀) (10 g, 5 mmol) was dissolved

in a stirring solution of THF (400 mL) to which 4-nitrophenyl chloroformate (2.01 g, 10 mmol) and triethylamine (1.39 mL, 10 mmol) were added. The solution was stirred for 2 days, the THF was removed under reduced pressure, and the crude product was resuspended in toluene (100 mL). The salt impurities were removed via filtration, and the final product was precipitated from toluene with copious amounts of ether. The white precipitate was dried to yield 4.68 g (2.1 mmol, 43%) of activated MPEG₂₀₀₀, and proton assignments matched those previously reported in the literature. ¹H NMR (CDCl₃, δ): 3.36 (s, OCH₃), 3.44 (m, CH₂OCH₃), 3.52 (m, COOCH₂CH₂O), 3.55–3.75 (br, OCH₂CH₂O), 3.79 (m, OCH₂CH₂OCH₃), 4.41 (dd, COOCH₂CH₂O), 7.48 (d, aromatic), 8.25 (d, aromatic).

DAB-Ac₄₀-PEG₄-FITC₂ (3). Activated MPEG₂₀₀₀ (443 mg, 0.2 mmol) was added to 5 mL of product solution containing dendrimer **1** to covalently attach long poly(ethylene glycol) chains to the remaining primary amines on the fluorescently labeled dendrimer. The solution was stirred for 24 h in the dark, concentrated under reduced pressure, resuspended in water, and dialyzed in a Spectra/Por Float-A-Lyzer (10 mL, 5000 MWCO) against 2 L of 0.5 M NaCl for 24 h, followed by dialysis in ultrapure Milli-Q water for 3 days (3 \times 2 L). The aqueous sample was frozen and lyophilized to yield 143 mg of an orange solid: ¹H NMR (D₂O, δ): 1.39–1.78 (m, NCH₂CH₂CH₂N, NCH₂CH₂CH₂CH₂N), 1.87 (s, COCH₃), 2.2–2.65 (m, NCH₂CH₂CH₂N, NCH₂CH₂CH₂NH), 2.84 (m, NCH₂CH₂CH₂NH₂), 3.07 (m, NCH₂CH₂CH₂NHCO-PEG), 3.28 (s, OCH₃), 3.41 (m, CH₂OCH₃), 3.50–3.70 (br, OCH₂CH₂O), 3.78 (m, OCH₂CH₂OCH₃), 4.09 (m, NHCOOCH₂CH₂O), 4.23 (m, NHCOOCH₂CH₂O). ESI-MS (unable to resolve a high molecular weight species with identical sampling procedure).

Ninhydrin Assay for Detection of Free Amines. The following procedure was adapted from Sarin et al. and uses the reagents in a standard commercially available Kaiser test kit.²⁸ Dendrimer samples were diluted to 3 μ M in absolute EtOH (n = 4 dilutions) and 700 μ L was added to a quartz cuvette, followed by 50 μ L of phenol (80% in ethanol), 50 μ L KCN in H₂O/pyridine, and 25 μ L of ninhydrin (6% in EtOH). The solutions were capped and heated at 100 $^{\circ}$ C for 10 min, and the spectroscopic absorption maxima of the Ruhemanns blue chromophore was measured at 570 nm via absorption spectroscopy. Absorbance values for dendrimers **1–3** were averaged (n = 4), normalized to the absorption maxima of the FITC chromophore (λ_{max} = 504 nm) as an internal standard, and compared to the ninhydrin response of 3 μ M G4-PAMAM possessing 64 exterior amines at the surface. Values represent the number of remaining amines per mole of dendrimer conjugate and are given as the standard deviation of the mean. **1** (DAB-Ac₄₀-FITC₂) = 24.9 \pm 4.9, **2** (DAB-Ac₅₉-FITC₂) = 3.7 \pm 1.5, **3** (DAB-Ac₄₀-PEG₄-FITC₂) = 21.2 \pm 5.5.

Cell Culture. Human umbilical vein endothelial cells (HUVEC) were purchased from Genlantis (catalog no. PH200050N, Genlantis Inc., CA) and propagated in Genlantis's serum containing endothelial growth medium (catalog no. PM 211500) according to the manufacturer's protocol.

Propidium Iodide (PI) Viability Assay. HUVEC were plated on 24-well tissue culture treated dishes (BD Bioscience #353047) at a density of 3.0 \times 10⁵ cells/mL (150 \times 10³ cells/well) and incubated overnight at 37 $^{\circ}$ C, in 5% CO₂/95% air for 18–20 h. For the PI assay, the incubation buffer was aspirated from each of the wells and replaced with 500 μ L of Krebs-Ringer-HEPES (KRH) buffer containing (mM): 115 NaCl, 5 KCl, 1 CaCl₂, 1 KH₂PO₄, 1.2 MgSO₄, 25 HEPES, pH 7.4, supplemented with 30 μ M of PI. The fluorescence of the cells in the absence and/or presence of 3 μ M dendrimer conjugates (**1**, **2**, or **3**) was monitored using a FluoStar Galaxy plate reader (BMG Labtech, Durham, NC) with excitation and emission filters set at 544 and 640 nm, respectively. Fluorescence was acquired at 15 min intervals for a total of 150 min. An additional 20 min incubation of cells with 40 μ M digitonin was required to completely permeabilize not only plasma membrane of HUVEC but also other internal membranes (including nuclear envelope). These conditions guarantee full access of PI to intracellular nucleic acids for achieving a maximum PI fluorescence.

Cell viability was presented as increase in PI fluorescence from each well expressed as percentage of maximal obtained in cells treated with digitonin (100% cell death).

Lactate Dehydrogenase (LDH) Assay. Twenty microliter aliquots of incubation buffer were removed from the plate used for the PI assay and stored at -20°C in black 96-well plates (Greiner, Monroe, NC) for subsequent LDH assays. Briefly, 96-well plates containing aliquots of incubation buffer were warmed to 37°C and LDH activity was measured from the rate of NADH production after adding $180\ \mu\text{L}$ of the buffer containing (mM): 0.22 NAD^{+} , 11.1 sodium lactate and 11.1 hydrazine, pH 8.0 into each well.²⁹ The kinetics of NADH fluorescence was monitored using a FluoStar Galaxy plate reader using 340 nm excitation and 460 nm emission filters. The LDH activity was expressed as the rate of relative fluorescence units per minute per well. Results were normalized to maximal LDH activity in each well obtained from samples treated with $40\ \mu\text{M}$ of digitonin for 20 min.

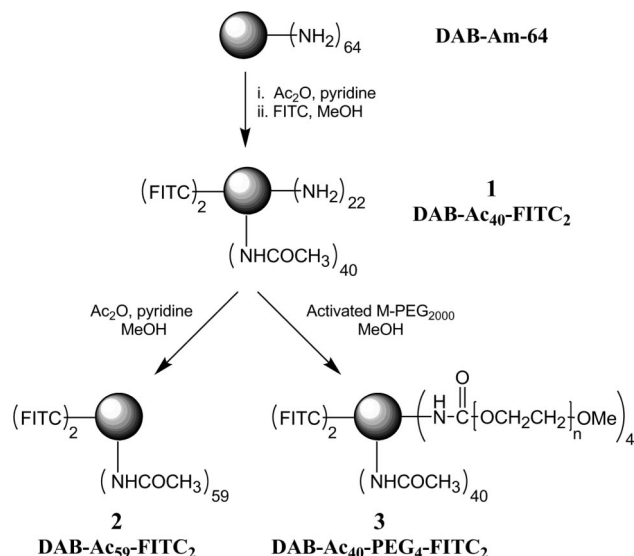
Imaging with Laser Scanning Confocal Microscopy. For confocal microscopy study HUVEC (3.0×10^5 cells/mL) were plated on round glass slides (Fisher Scientific, Pittsburgh, PA) and incubated overnight in 1 mL of Genlantis' growth medium at 37°C , 5% CO_2 in a humidified environment. The cells on the coverslip were preloaded with TMRM, a mitochondria specific fluorescent dye (100 nM, for 30 min at 37°C) and placed into an environmental chamber (37°C , 5% CO_2 , 100% humidity) of the stage of fluorescent confocal microscope Zeiss LSM 510 (Carl Zeiss, Thornwood, NY). Incubation medium was replaced with 1 mL of KRH buffer containing $30\ \mu\text{M}$ PI and $3\ \mu\text{M}$ FITC-dendrimer and confocal images of HUVEC were acquired every 5 min for 30 min total using a $63\times$ N.A. 1.4 planapochromat oil immersion lens with pinholes set to 1.0 Airy units in both the red (TMRM) and green (FITC) channels. Fluorophores were excited with the 543 nm line of a HeNe laser (TMRM) and the 488 nm line of an Ar laser (FITC), with laser intensities attenuated to 0.05%. Green and red fluorescence were separated by a dichroic filter (NFT 545) and recorded in channels 2 and 3 of the LSM 510 using band-pass (BP 500–530) and long-pass (LP 560) filters, respectively. (Fluorophore absorption/emission spectra provided by manufacturer and dendrimer absorption spectra may be found in Supporting Information).

Statistics. Differences between the effects of dendrimers on cultured cells were analyzed using one-way ANOVA with Fisher's multiple comparisons post hoc test, $p < 0.05$ as the criterion of significance. All experiments were repeated at least three times, and results were expressed as means \pm SEM. When error bars are not shown, they fall within the diameters of the symbols.

Results and Discussion

Synthesis and Characterization of Dendrimer Conjugates. Generation 5 polypropylenimine dendrimer (DAB-Am-64) was chosen as the starting material due to its previously reported toxicity in drug delivery applications and its capacity for a large number of additional functionalities.^{4,18} The cytotoxicity of DAB-Am-64 and other amine-containing dendrimers is mediated by nonspecific interactions of the positively charged primary amines with lipid membranes.²² Therefore, we stoichiometrically targeted half of the surface positive charges on the parental dendrimer (DAB-Am-64) for conversion into acetamides via reaction with acetic anhydride (Scheme 1). Previously, amide dendritic exteriors have been used to increase water solubility and eliminate the toxicity of primary amine dendrimer constructs.^{19,30} The partially acetylated product was then fluorescently labeled with FITC to produce a fully traceable dendrimer conjugate **1** (Scheme 1, DAB-Ac₄₀-FITC₂) for studying the interaction of mixed amine/amide dendrimers with cultured cells. Fluorescent labeling of dendrimer drug delivery scaffolds enables the direct monitoring of cellular interactions in vitro and also imparts a molecular probe to study future

Scheme 1. Synthesis of Multifunctional Dendrimer Conjugates (DAB-Am-64, parental unmodified generation 5 polypropylenimine dendrimer; FITC, fluorescein isothiocyanate)



biodistribution in vivo.^{10,31} The modified dendrimer was dialyzed for 96 h, lyophilized, and analyzed via nuclear magnetic resonance spectroscopy (^1H NMR) and electrospray ionization mass spectrometry (ESI/MS). The extent of amide functionalization (40 of 64 amines) was calculated from molecular weight and the integration ratio of the protons on the newly formed amide (COCH_3) to the aliphatic methylene protons of the dendritic interior. The integrated ratio of the aromatic protons on the fluorophore to the protons alpha to the exterior amine (CH_2NH_2) indicated an average of two FITC residues per dendrimer (Supporting Information).

The remaining exterior amines of the partially acetylated and FITC-labeled dendrimer **1** (DAB-Ac₄₀-FITC₂) were further modified as shown in Scheme 1. Dendrimer **1** was reacted with either excess acetic anhydride to fully acetylate the dendrimer surface yielding dendrimer **2** (DAB-Ac₅₉-FITC₂) or with 4-nitrophenyl poly(ethylene glycol) monomethylether (activated M-PEG₂₀₀₀) following a previously reported procedure²⁷ to yield PEG-ylated dendrimer **3** (DAB-Ac₄₀-PEG₄-FITC₂). Dendrimer conjugates **1–3** thereby provide a unique set of fluorescently labeled macromolecules, comprising defined percentages of amine, amide, or PEG modification, from which to study dendrimer induced cytotoxicity *in vitro*. A quantitative ninhydrin assay was then conducted on the dendrimers to determine the number of free amines per molecule of dendrimer.²⁸ Dendrimer **1** retained 24.9 ± 4.9 primary amines after partial acetylation, dendrimer **2** contained 3.7 ± 1.5 remaining amines after full acetylation, and PEG modified dendrimer **3** possessed 21.2 ± 5.5 solvent accessible amines after coupling of the activated PEG moieties, indicating attachment of ~ 4 hydrophilic PEG chains. The quantification of amines *per* dendrimer molecule correlated with the number of amines predicted from NMR and ESI-MS data analysis (**1** = 22 NH_2 ; **2** = 3 NH_2 ; **3** = 18 NH_2); in all cases the predicted number of remaining amines was within the error of the number of amines determined via the colorimetric assay.

Cytotoxicity of Dendrimer Conjugates. The toxicity of amine-containing dendrimer constructs has been studied against a range of target tissue cell lines from hamster ovarian cells¹⁴ to human embryonic kidney cells.³² However, upon systemic administration of a delivery system, the therapeutic first comes

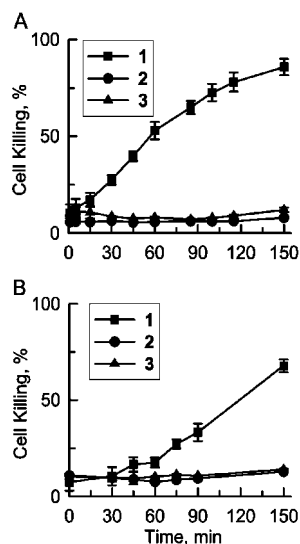


Figure 1. Cytotoxicity of dendrimer conjugates in cultured HUVEC. (A) Time dependent cell killing as evaluated using PI assay: (■) dendrimer 1 (DAB-Ac₄₀-FITC₂), (●) dendrimer 2 (DAB-Ac₅₉-FITC₂), (▲) dendrimer 3 (DAB-Ac₄₀-PEG₄-FITC₂). (B) Time dependence of dendrimer-mediated release of LDH from cultured HUVEC: (■) dendrimer 1 (DAB-Ac₄₀-FITC₂), (●) dendrimer 2 (DAB-Ac₅₉-FITC₂), (▲) dendrimer 3 (DAB-Ac₄₀-PEG₄-FITC₂). The data are means \pm SEM of three independent experiments.

into contact with the endothelium which ultimately mediates the delivery of the drug to other tissues.^{33,34} The present study evaluates the cytotoxicity of the dendrimer conjugates toward cultured human umbilical vein endothelial cells (HUVEC) as a model of the intravascular lining that first interacts with dendrimer delivery vehicles upon intravenous injection. Additionally, endothelial cells are a primary target for gene therapies used to treat many cardiovascular conditions including restenosis and myocardial ischemia.²⁶

To assess the cytotoxicity of the various dendrimer conjugates, HUVEC were plated to 85% confluency in 24-well plates and treated with dendrimer conjugates (3 μ M) in KRH buffer containing 30 μ M propidium iodide (PI). In cultures possessing healthy cells with intact membranes, PI is nonfluorescent and does not enter the cell. When the plasma membrane is compromised, PI diffuses into the cell and binds to nuclear chromatin, producing an increase in red fluorescence.^{35,36} The viability of HUVEC was calculated from the observed PI fluorescence intensity normalized to the maximum values achieved after complete permeabilization of the plasma membranes of the entire HUVEC population with digitonin (40 μ M), a recognized nonionic detergent that solubilizes membrane-bound cholesterol leaving nonselective pores in biological membranes.³⁷

HUVEC treated with 3 μ M dendrimer 1 (DAB-Ac₄₀-FITC₂) exhibited rapid changes in plasma membrane permeability as evidenced by the sharp increase in PI fluorescence after only 30 min (Figure 1A). The rise is indicative of substantial acute toxicity of this agent. After 150 min, the fluorescence signal began to plateau and >90% of the cells in culture were dead. The temporal dynamics of plasma membrane disruption by dendrimer 1 was further confirmed by measuring the release of LDH, a cytosolic enzyme, from the same cells. As shown in Figure 1B, the LDH activity from aliquots of the incubation buffer also increased over time after exposure to dendrimer 1 but at a slight delay compared to the passage of the smaller PI. Notably, the PI assay demonstrated more than 50% cell death

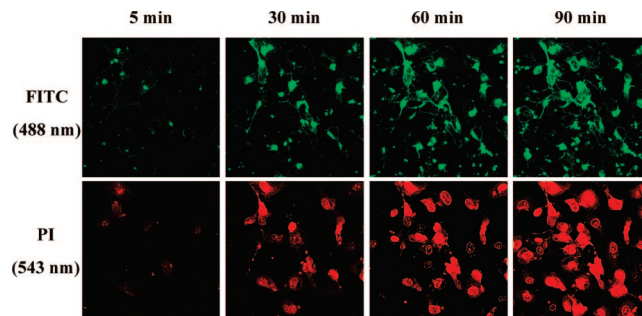


Figure 2. Confocal fluorescence microscopy images of the time-dependent membrane permeability changes of HUVEC exposed to 3 μ M amine containing dendrimer 1 in culture media containing 30 μ M PI.

after 60 min of dendrimer exposure, while the LDH release reached only 20% of the maximum. Therefore, the release of LDH initiated by amine-containing dendrimers occurred at longer incubation times than the increase in PI fluorescence from the same cells, indicating that the size of the holes in the plasma membrane increased progressively with time; cells first became permeable to the 698 Da PI molecules and later to the 140 kDa LDH enzyme. Both assays clearly indicate that amine-containing dendrimer 1 caused permeabilization and disruption of the plasma membrane integrity in a time-dependent fashion, thus confirming that dendrimers with cationic amines at their surfaces are cytotoxic and that partial acetylation is insufficient at eliminating the deleterious effects of amine-presenting delivery vehicles. These data provide experimental validation to the molecular dynamics simulations reported by Larson and co-workers that suggest pore formation can be induced by 50% acetylated PAMAM dendrimers on simulated DPPC bilayers.²¹

The viability of HUVEC exposed to 3 μ M dendrimers 2 and 3 is also shown in Figure 1. No observable cytotoxicity was detected for either dendrimer using the PI (Figure 1A) or LDH (Figure 1B) assays and there was no statistical differences between the effect of dendrimers 2 and 3 ($p = \text{NS}$). After 150 min of incubation of HUVEC, the level of PI labeling and LDH release remained unchanged from initial levels, indicating that the fully amidated and PEG-modified exteriors did not disrupt the plasma membrane integrity. These data are in accord with the previously observed enhancement of dendrimer's biocompatibility through modification of surface functionalities.^{14,22,32,38}

Confocal Laser Scanning Microscopy of Dendrimer Interactions with HUVEC. Disruption of the Plasma Membrane Integrity by Amine-Containing Dendrimers. The exact mechanism of gene transfection for cationic dendrimers is unknown, but the ability to disrupt the plasma membrane and induce hold formation as previously described resembles the physical process by which other nonviral transfection agents induce pores to deliver DNA cargo (e.g., lipofectamine).^{39,40} Interaction of the cationic delivery vehicle with the membrane is essential, but large disruptions may cause an influx of extracellular fluid and initiate a cascade of apoptotic events including the depolarization of intracellular mitochondria.

To visually monitor the time-dependent changes in membrane permeability, HUVEC were cultured onto glass slides in KRH buffer containing 30 μ M propidium iodide (PI), treated with dendrimer conjugates (3 μ M), and imaged via confocal fluorescence microscopy. Fluorescent labeling of the dendrimer conjugates enabled direct visualization of the interaction between the dendrimer and the plasma membrane of cultured cells. Figure 2 depicts HUVEC exposed to the partially modified, amine-containing dendrimer 1. After 30 min, fluorescently labeled

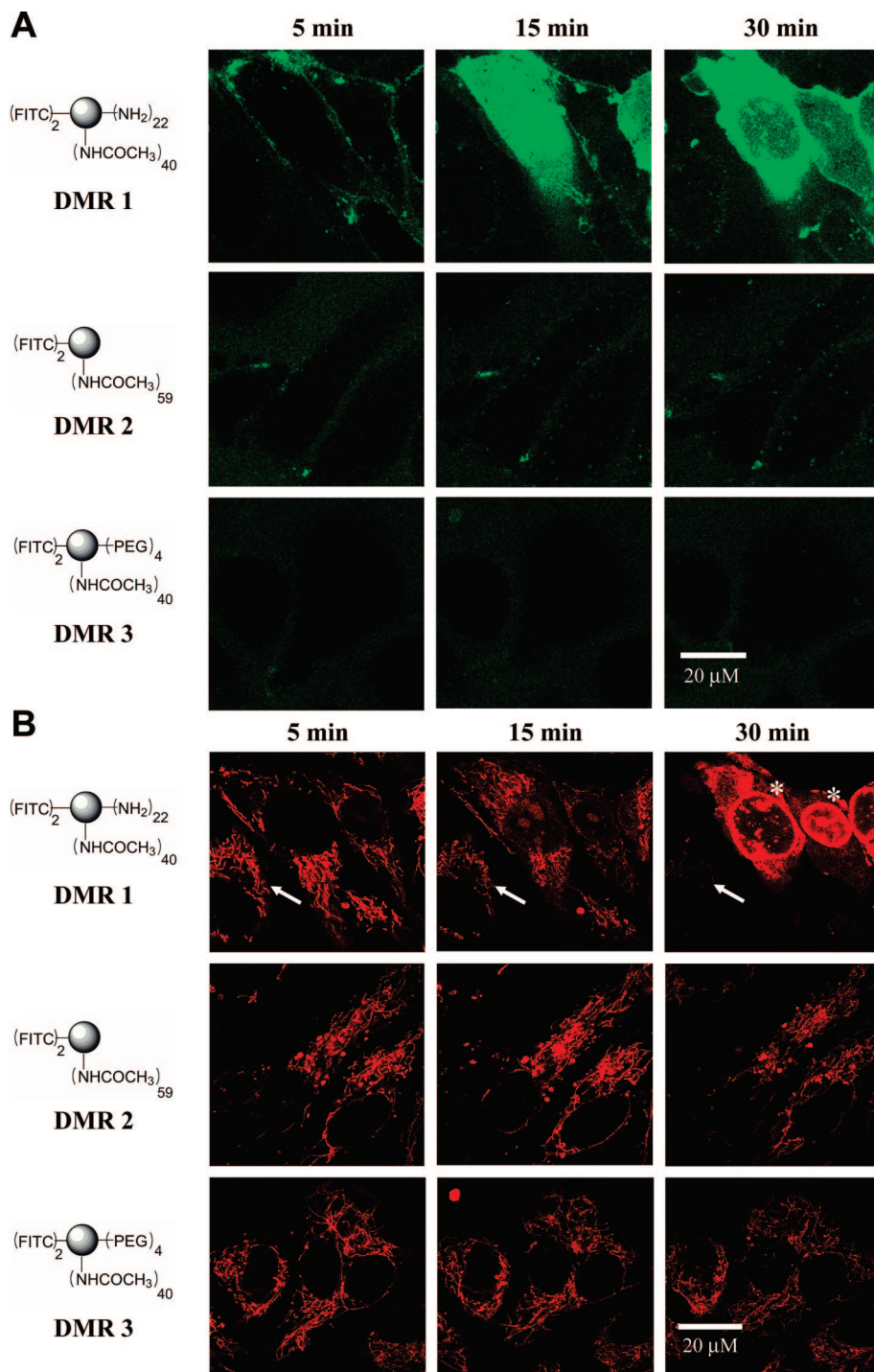


Figure 3. The effect of dendrimers 1–3 on cultured endothelial cells. Confocal images of HUVEC treated with 3 μM fluorescent dendrimer conjugate (A, green top panels) coloaded with TMRM (B, red bottom panels) in KRH buffer supplemented with 30 μM of PI. Amine-containing dendrimer 1 adhered and completely outlined the plasma membrane of most cells within 5 min. Further incubation revealed a large intracellular green fluorescence which paralleled the progressive loss of mitochondrial membrane potential (decrease in TMRM fluorescence, white arrows) and entrance of PI into the cells at 15 and 30 min (white asterisks denote typical red fluorescence of PI in the nuclei). Note that even after 30 min of incubation with dendrimers 2 and 3 there is no significant dendrimer adherence to the plasma membrane, depolarization of mitochondria, or PI entrance into the nuclei.

dendrimer 1 appeared to completely permeate the plasma membrane and progressively accumulate within the intracellular compartment, via either diffusion through newly formed holes or an endocytotic mechanism proposed previously for other dendrimer conjugates.⁴¹ A rapid increase in the number of red fluorescent nuclei was also observed, visually confirming the kinetics of PI uptake as shown in Figure 1. The sequence of images (Figure 2) clearly illustrates that increases

in red fluorescence (PI uptake) coincide with the increase of the green fluorescence (dendrimer uptake) throughout the entire cell population. In the absence of dendrimers, cells retained their viability for up to 90 min and confocal images demonstrated no significant increase in red fluorescence of PI over the time course of the experiment (data not shown). In similar experimental setup, exposure of HUVEC cells to dendrimer conjugate 2 or 3 resulted in no appreciable increase

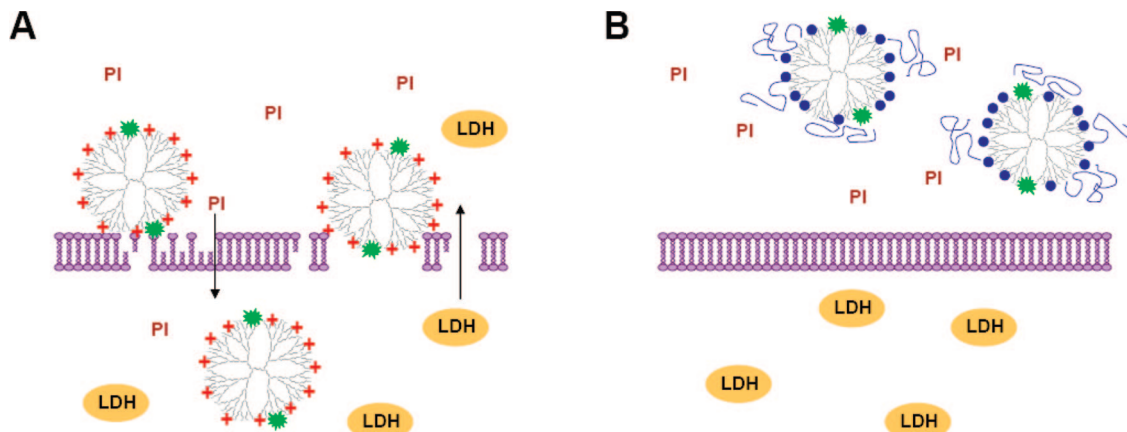


Figure 4. Illustration of dendrimers interacting with the plasma membrane of cultured cells. (A) Primary amine containing dendrimer **1** (DAB-Ac₄₀-FITC₂) induces hole formation and allows the transport of dendrimer, PI, and LDH across the plasma membrane. (B) Amide/PEG modified dendrimer **3** (DAB-Ac₄₀-PEG₄-FITC₂) exhibits no membrane disruption or intracellular accumulation monitored via fluorescence-based techniques.

in PI fluorescence, consistent with the PI and LDH cytotoxicity assays (Figure 1).

Cellular Adhesion of Dendrimers 1–3 and Mitochondrial Depolarization. The series of confocal microscopy images shown in Figure 3 illustrates the time-dependent changes in HUVEC viability after addition of the dendrimer conjugates. Upon exposure of cells to FITC-labeled amine-terminated dendrimer **1** for 5 min, a bright, punctuated green outline of the cells was observed, indicating adherence of FITC-dendrimer to the plasma membrane (Figure 3A, DMR 1). Although imaged simultaneously, the origins of the PI and TMRM fluorescence are different. Here, imaging of PI and TMRM (both were excited using 543 nm laser line and red fluorescence was acquired through LP560 filter) was intended to demonstrate that the collapse of mitochondrial membrane potential (punctate structures within the cells) occurs before increased characteristic PI fluorescence responsible for nuclear staining (large oval rings filled with fragmented red patches) as shown in Figure 3, 30 min. The cellular interactions of fluorescently labeled dendrimers **2** and **3** were also examined using the same protocols as for FITC-labeled dendrimer **1** but no appreciable accumulation of the green fluorescence was observed on the membrane of HUVEC in culture (Figure 3A, DMR 2 and DMR 3). Thus, chemical conversion of cationic amines at the dendrimer surface to amides or sterically shielding the cationic surface via attached hydrophilic PEG chains resulted in substantial loss of the polymer's adhesion to the plasma membranes of HUVEC. Even at longer incubation times (>60 min) no significant accumulation at the membrane was observed for either the amide or PEG-modified dendrimer conjugate.

To probe the effects of dendrimers on the membrane potential of intracellular mitochondria, cells were loaded with 100 nM TMRM dye prior to imaging. The cationic dye is retained in the mitochondria with high membrane potential indicative of cell viability, whereby compromised cells undergo a characteristic loss of mitochondrial membrane potential and a disappearance of red fluorescent staining.⁴² Confocal images of endothelial cells with TMRM-labeled mitochondria exposed to FITC-labeled dendrimers are shown in Figure 3B. At early time points (5 min) of treatment with any of the dendrimer conjugates intracellular mitochondria retain TMRM dye in the matrix. After 15 min of exposure to dendrimer **1**, the plasma membrane of cultured cells no longer retained its integrity as evidenced by the decrease in red mitochondrial fluorescence (white arrows)

and a slow influx of extracellular PI into the cell nuclei (Figure 3B, DMR 1). Complete loss of TMRM fluorescence from mitochondria coincided with the staining of the nuclear envelope (white asterisks) and loss cell viability that occurred at 30 min of exposure to dendrimer **1**. In control experiments we demonstrated that TMRM, a mitochondria selective fluorescent dye, does not bind to cell nuclei, and vice versa, PI does not label mitochondria in cells with compromised plasma membranes (Supporting Information).

Mitochondrial depolarization may be the result of a dramatic increase in cytosolic Ca²⁺ concentration due to the loss of plasma membrane integrity and influx of extracellular Ca²⁺.⁴³ Correspondingly, no visible mitochondrial depolarization or PI staining of the nuclei was observed upon exposure of cultured cells to the FITC-labeled dendrimers **2** or **3** (Figure 3B, DMR 2 and DMR 3). The TMRM fluorescence appeared to be unchanged over 30 min, indicating preservation of the mitochondrial membrane potential and minimal damage to the cellular plasma membrane. Despite the solvent accessible amines still available on dendrimer conjugate **3** (ninhydrin assay, Scheme 1), the 2000 MW PEG chains proved to be sufficient to block the cationic surface from interacting with the negatively charged membranes of endothelial cells. Thus, preventing the interaction between the cationic dendrimer surface and the plasma membrane of endothelial cells appears to be a necessary step in eliminating the cytotoxicity of dendrimer delivery vehicles.

Conclusion

Figure 4 summarizes our results obtained in the fluorescent viability assays and confocal microscopy experiments. Cationic amine residues at the surface of polypropylenimine dendrimers induced drastic and time-dependent changes in HUVEC membrane permeability toward cytosolic enzymes and PI (Figure 4A). Rapid cellular uptake of PI, a low molecular weight dye, was detected as early as 15 min, and the larger cytosolic proteins (e.g., LDH) were released from the cells at later time points. Alteration of amines to amides or covalent attachment of PEG resulted in dendrimer conjugates containing mixed functionalities with no acute toxicity profiles (Figure 4B). The data presented herein are in agreement with the reported cytotoxicity of amine-terminated dendrimers and strongly suggest that primary-amine-terminated dendrimers should be avoided as drug

delivery vehicles. In conclusion, the cytotoxicity and biocompatibility of dendrimer vehicles is dependent on the surface composition, and it is essential that dendrimer-based drugs formulated for intravenous injection be tested for specific cytotoxicity toward endothelial cells.

Acknowledgment. This research was funded by the North Carolina Biotechnology Center (Grant 20006-MRG-1116), Pfizer Analytical Graduate Fellowship to Nate Stasko, and the University of North Carolina—Chapel Hill's E.C. Markham Summer Research Award to C. Bryce Johnson. We thank Dr. Matt Crowe of the Department of Chemistry Mass Spectrometry Facility at the University of North Carolina—Chapel Hill (Chapel Hill, NC) for product analysis.

Supporting Information Available. Representative NMR spectra for characterizing dendrimer conjugates and the confocal fluorescence microscopy images of control experiments in cultured HUVEC. This material is available free of charge via the Internet at <http://pubs.acs.org>.

References and Notes

- (1) Stiriba, S.-E.; Frey, H.; Haag, R. *Angew. Chem., Int. Ed.* **2002**, *41*, 1329–1334.
- (2) Svenson, S.; Tomalia, D. A. *Adv. Drug Delivery Rev.* **2005**, *57*, 2106–2129.
- (3) Frechet, J. M. J. *Polym. Sci., A: Polym. Chem.* **2003**, *41*, 3713–3725.
- (4) Boas, U.; Heegaard, P. M. H. *Chem. Soc. Rev.* **2004**, *33*, 43–63.
- (5) Gillies, E. R.; Frechet, J. M. *Drug Discovery Today* **2005**, *10*, 35–43.
- (6) Meijer, E. W.; Jansen, J.; Brabander-van den Berg, E. *Science* **1994**, *266*, 1226–1229.
- (7) Morgan, M. T.; Carnahan, M. A.; Immoos, C. E.; Ribeiro, A. A.; Finkelstein, S.; Lee, S. J.; Grinstaff, M. W. *J. Am. Chem. Soc.* **2003**, *125*, 15485–15489.
- (8) Patri, A. K.; Myc, A.; Beals, J.; Thomas, N. H.; Baker, J. R., Jr. *Bioconjugate Chem.* **2004**, *15*, 1174–1181.
- (9) Kukowska-Latallo, J. F.; Candido, K. A.; Cao, Z.; Nigavekar, S. S.; Majoros, I. J.; Thomas, T. P.; Balogh, L. P.; Khan, M.; Baker, J. R., Jr. *Cancer Res.* **2005**, *65*, 5317–5324.
- (10) Majoros, I. J.; Myc, A.; Thomas, T.; Mehta, C. B.; Baker, J. R., Jr. *Biomacromolecules* **2006**, *7*, 572–579.
- (11) Dufes, C.; Uchegbu, I. F.; Schatzlein, A. G. *Adv. Drug Delivery Rev.* **2005**, *57*, 2177–2202.
- (12) Kubasiak, L. A.; Tomalia, D. A. Cationic dendrimers as gene transfection vectors: dendri-poly(amidoamines) and dendri-poly(propyleneimines). In *Polymeric Gene Delivery*; Amiji, M. M., Ed.; CRC Press LLC: Boca Raton, FL, 2005; pp 133–157.
- (13) Haensler, J.; Szoka, F. C. Jr. *Bioconjugate Chem.* **1993**, *4*, 372–379.
- (14) Luo, D.; Haverstick, K.; Belcheva, N.; Han, E.; Saltzman, W. M. *Macromolecules* **2002**, *35*, 3456–3462.
- (15) Braun, C. S.; Vetro, J. A.; Tomalia, D. A.; Koe, G. S.; Koe, J. G.; Middaugh, C. R. *J. Pharm. Sci.* **2005**, *94*, 423–436.
- (16) Bielinska, A. U.; Chen, C.; Johnson, J.; Baker, J. R., Jr. *Bioconjugate Chem.* **1999**, *10*, 843–850.
- (17) Bielinska, A. U.; Kukowska-Latallo, J. F.; Baker, J. R., Jr. *Biochim. Biophys. Acta* **1997**, *1353*, 180–190.
- (18) Duncan, R.; Izzo, L. *Adv. Drug Delivery Rev.* **2005**, *57*, 2215–2237.
- (19) Hong, S.; Bielinska, A. U.; Mecke, A.; Keszler, B.; Beals, J. L.; Shi, X.; Balogh, L.; Orr, B. G.; Baker, J. R., Jr. *Bioconjugate Chem.* **2004**, *15*, 774–782.
- (20) Mecke, A.; Majoros, I. J.; Patri, A. K.; Baker, J. R. Jr.; Banaszak-Holl, M. M.; Orr, B. G. *Langmuir* **2005**, *21*, 10348–10354.
- (21) Lee, H.; Larson, R. G. *J. Phys. Chem. B* **2006**, *110*, 18204–18211.
- (22) Hong, S.; Leroueil, P. R.; Janus, E. K.; Peters, J. L.; Kober, M.-M.; Islam, M. T.; Orr, B. G.; Baker, J. R., Jr.; Banaszak-Holl, M. M. *Bioconjugate Chem.* **2006**, *17*, 728–734.
- (23) Fuchs, S.; Kapp, T.; Otto, H.; Schoneberg, T.; Franke, P.; Gust, R.; Schluter, A. D. *Chem. Eur. J.* **2004**, *10*, 1167–1192.
- (24) Jevprasesphant, R.; Penny, J.; Attwood, D.; McKeown, N. B.; D'Emanuele, A. *Pharm. Res.* **2003**, *20*, 1543–1550.
- (25) Tack, F.; Bakker, A.; Maes, S.; Dekeyser, N.; Bruining, M.; Elissen-Roman, C.; Janicot, M.; Brewster, M.; Janssen, H. M.; De Waal, B. F. M.; Fransen, P. M.; Lou, X.; Meijer, E. W. *J. Drug Targeting* **2006**, *14*, 69–86.
- (26) Green, J. J.; Shi, J.; Chiu, E.; Leshchiner, E. S.; Langer, R.; Anderson, D. G. *Bioconjugate Chem.* **2006**, *17*, 1162–1169.
- (27) Kojima, C.; Kono, K.; Maruyama, K.; Takagishi, T. *Bionconjugate Chem.* **2000**, *11*, 910–917.
- (28) Sarin, V. K.; Kent, S. B. H.; Tam, J. P.; Merrifield, R. B. *Anal. Biochem.* **1981**, *117*, 147–157.
- (29) Puranam, K. L.; Boustany, R.-M. Assessment of cell viability and histochemical methods in apoptosis. *Apoptosis in Neurobiology*; Hannun, Y. A., Boustany, R.-M., Eds.; CRC Press LLC: Boca Raton, FL, 1998; 129–152.
- (30) Majoros, I. J.; Keszler, B.; Woehler, S.; Bull, T.; Baker, J. R., Jr. *Macromolecules* **2003**, *36*, 5526–5529.
- (31) Marano, R. J.; Toth, I.; Wimmer, N.; Brankov, M.; Rakoczy, P. E. *Gene Ther.* **2005**, *12*, 1544–1550.
- (32) Kim, T.; Seo, H. J.; Choi, J. S.; Jang, H.-S.; Baek, J.; Kim, K.; Park, J.-S. *Biomacromolecules* **2004**, *5*, 2487–2492.
- (33) Chappey, O.; Wautier, M. P.; Wautier, J. L. *Toxicol. in Vitro* **1995**, *9*, 411–419.
- (34) Vane, J. R.; Anggard, E. E.; Botting, R. M. *N. Engl. J. Med.* **1990**, *323*, 27–36.
- (35) Gores, G. J.; Nieminen, A.-L.; Fleishman, K. E.; Dawson, T. L.; Herman, B.; Lemasters, J. J. *Am. J. Physiol.* **1988**, *255*, 315–322.
- (36) Lemasters, J. J.; DiGuiseppi, J.; Nieminen, A.-L.; Herman, B. *Nature* **1987**, *325*, 78–81.
- (37) Becker, G. L.; Fiskum, G.; Lehninger, A. L. *J. Biol. Chem.* **1980**, *255*, 9009–9012.
- (38) Jevprasesphant, R.; Penny, J.; Jalal, R.; Attwood, D.; McKeown, N. B.; D'Emanuele, A. *Int. J. Pharm.* **2003**, *252*, 263–266.
- (39) Felgner, P. L.; Gadek, T. R.; Holm, M.; Roman, R.; Chan, H. W.; Wenz, M.; Northrop, J. P.; Ringold, G. M.; Danielsen, M. *Proc. Natl. Acad. Sci. U.S.A.* **1987**, *84*, 7413–7417.
- (40) Horobin, R. W.; Weissig, V. *J. Gene Med.* **2005**, *7*, 1023–1034.
- (41) Kolhe, P.; Khandare, J.; Pillai, O.; Kannan, S.; Lieh-Lai, M.; Kannan, R. M. *Biomaterials* **2006**, *27*, 660–669.
- (42) Kim, J.-S.; Ohshima, S.; Padiaditakis, P.; Lemasters, J. J. *Hepatology* **2004**, *39*, 1533–1543.
- (43) Sedova, M.; Dedkova, E. N.; Blatter, L. A. *Am. J. Physiol. Cell Physiol.* **2006**, *291*, 840–850.

BM7008203